

Constraining the annihilation of dark matter via cosmic-ray positrons and electrons

Suwitchaya Setthahirun¹ and Maneenate Wechakama^{1,2,*}

¹Department of Physics, Faculty of Science, Kasetsart University, Bangkok, 10900, Thailand

²National Astronomical Research Institute of Thailand (Public Organization), Chiangmai, 50180, Thailand

*E-mail: fscimnw@ku.ac.th

Abstract. We aim to constrain the properties of dark matter particles by several measurements of positrons and electrons from cosmic-rays. We assume that collisions of dark matter particles and dark matter anti-particles can produce positrons and electrons. The electron-positron propagation is explained by a diffusion-loss equation including loss rates, diffusion, as well as source function. We use data of cosmic-ray positrons and electrons detected by PAMELA, H.E.S.S., AMS-02 and Fermi-LAT. We compare the observational data with the electron and positron spectrum from five annihilation channels in our model to derive constraining factors regarding the cross-section of the annihilation of dark matter. The tightest constraint is provided by cosmic-ray positrons of AMS-02 for the electron channel. Dark matter with mass below a few GeV gets excluded by the cosmic-ray positrons of AMS-02 for the electron, muon and tau channels.

1. Introduction

Dark matter properties can be examined by indirect detection based on the assumption that dark matter particles and dark matter anti-particles can collide and annihilate into positrons and electrons [1]. Several experiments have shown that electron and positron data exceeded the predicted astrophysical backgrounds in the solar neighbourhood [2]. This led to various attempts to detect their abnormalities which can be assumed to be the result of the annihilation of dark matter. Data regarding cosmic-ray electrons and positrons have been detected by several experiments; the Alpha Magnetic Spectrometer (AMS-02) [3], Fermi-Large Area Telescope (Fermi-LAT) [4–6], the Payload for Antimatter Matter Exploration and Light-nuclei Astrophysics (PAMELA) [7, 8]) as well as the High Energy Stereoscopic System (H.E.S.S.) [9].

Within this paper we aim to derive constraining factors of the cross-section of the annihilation of dark matter and masses of dark matter particles by using data from several experiments that detected cosmic-ray positrons and electrons. We examine positrons and electrons produced from quark and lepton channels of the annihilation of dark matter. Based on the result from a diffusion-loss equation, we aim to explain the spectrum of positrons and electrons taking loss rates, diffusion, and source term into consideration. The upper limits of the cross-section of the annihilation of dark matter are derived by comparing the observational electron and positron data to our model spectrum.

2. Method and data

2.1. Model predictions

Our model assumes that dark matter particles and dark matter anti-particles can annihilate into positrons and electrons through quark and lepton channels. The energy of positrons and electrons diminishes as a result of traveling through the Galaxy due to ionization with hydrogen atoms, inverse Compton scattering by photons with low energy and synchrotron radiation through magnetic fields. Assuming spherical symmetry; positron and electron propagation at r from the centre of the Galaxy can be expressed as a diffusion-loss equation as shown in [10] where the spectrum of electrons as well as positrons is given by

$$\frac{dn}{d\gamma}(r, \gamma) = \frac{1}{b(\gamma)} \frac{\exp\left(-\frac{r^2}{2\Delta\lambda^2}\right)}{(2\pi r^2 \Delta\lambda^2)^{1/2}} \times \left\{ \int_{\gamma}^{\infty} d\gamma_0 \int_0^{\infty} dr_0 r_0 \exp\left(-\frac{r_0^2}{2\Delta\lambda^2}\right) \times \left[\exp\left(\frac{rr_0}{\Delta\lambda^2}\right) - \exp\left(-\frac{rr_0}{\Delta\lambda^2}\right) \right] Q(r_0, \gamma_0) \right\}, \quad (1)$$

where γ is the Lorentz factor related to the energy $E = \gamma m_e c^2$ of the positrons and electrons, m_e represents the electron mass while at rest, c is the light speed constant, γ_0 and r_0 represent their initial energy and initial location where they are created, respectively. $\Delta\lambda^2 = \lambda^2(\gamma) - \lambda^2(\gamma_s)$, where λ is the positron and electron's diffusion length in a function of the coefficient of diffusion $K(\gamma)$ and energy loss-rate $b(\gamma)$, as given by

$$\lambda^2(\gamma) = \int_{\gamma}^{\infty} \frac{2K(\gamma)}{b(\gamma)} d\gamma. \quad (2)$$

We adopt the model of the energy loss rate and the coefficient of diffusion from [10] and [11], respectively.

The source term that represents the rate of the positron and electron production from the annihilation of dark matter is given by

$$Q(r, \gamma) = \frac{1}{2} \left[\frac{\rho_{\text{dm}}(r)}{m_{\text{dm}}} \right]^2 \langle \sigma v \rangle_{e^{\pm}} \frac{dN_{e^{\pm}}}{d\gamma} \delta(\gamma - \gamma_0), \quad (3)$$

where m_{dm} is the mass of dark matter particle, $\langle \sigma v \rangle_{e^{\pm}}$ is the average annihilation cross-section multiplied by the relative particle velocity of dark matter and its anti-particle equivalents. Given our assumption that particles of dark matter are Majorana particles, i.e. self-conjugate particles, we add a factor 1/2 to avoid double counting. We adopt the final state injection spectrum of positrons and electrons, $\frac{dN_{e^{\pm}}}{d\gamma}$, for each annihilating channel from PPPC4DMID including electroweak corrections [12, 13].

The question regarding profiling the density of dark matter distributed throughout the Milky Way is still not settled. Either the shape of the profile can be very steep at the inner regions due to the adiabatic contraction from gas and stars [14], or it can be shallower as suggested in, e.g., [15]. In our model, we use the most common universal profile for dark matter halos identified in N-body simulations by [16] a profile developed by Frenk, Navarro and White with a spherically-symmetric halo for the profile of dark matter density,

$$\rho_{\text{dm}}(r) = \frac{\rho_s}{\left(\frac{r}{r_s}\right) \left(1 + \frac{r}{r_s}\right)^2}, \quad (4)$$

where r_s and ρ_s are the characteristic density and radius of the halo of the Milky Way, respectively. The characteristic density $\rho_s c^2$ and radius r_s are equal to $0.349 \text{ GeV cm}^{-3}$ and 16.7 kpc respectively as shown in [17].

2.2. Electron and positron data

Data from several remarkable experiments such as AMS-02, PAMELA, H.E.S.S. as well as Fermi-LAT is used with the intention of constraining the properties of dark matter particles. The data from AMS-02 contain the flux for electrons within the energy span between 0.5 GeV to 700 GeV as well as flux for positrons within the energy span between 0.5 GeV to 500 GeV [3]. We further utilize the data about positrons and electrons from cosmic-rays provided by PAMELA, where the electron data are represented within the energy span between 1 GeV to 625 GeV [7] and the positron data are represented in the energy span between 1 GeV to 300 GeV, [8]. The observed spectra of positrons as well as electrons from cosmic-rays that were detected within Fermi-LAT in the energy span between 7 GeV to 1 TeV [5] are also used as well as the electron plus positron data with the energy span between 7 GeV to 2 TeV [6]. Finally, we use the high energy electron spectrum with energy above 600 GeV detected by H.E.S.S. [9]. All aforementioned data are shown in figure 1.

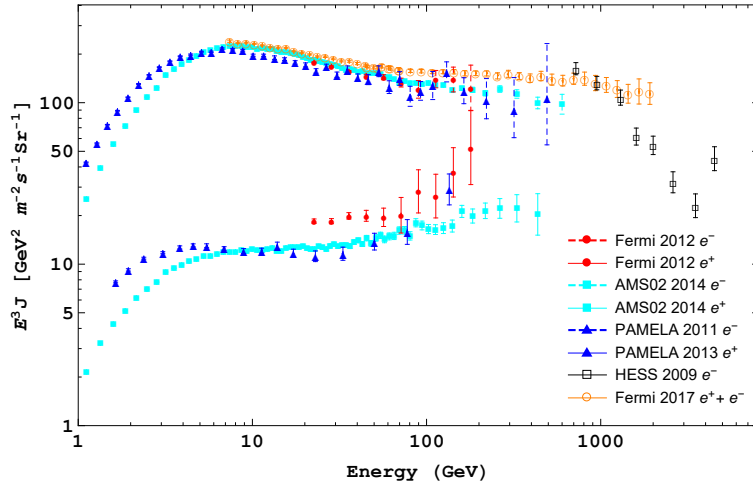


Figure 1. Spectrum of electron plus positron, only electron and only positron as measured by H.E.S.S., PAMELA, AMS-02 as well as Fermi-LAT.

3. Upper limits of the cross-section of the annihilation of dark matter

Our focus here is the property investigation regarding particles of dark matter, i.e. masses and the cross-section of annihilation. By comparing positron and electron data in the solar neighbourhood with electron and positron spectrum in our model, we can derive the upper limits of the cross-section of the annihilation of dark matter multiplied by the relative particle velocity of dark matter and dark matter anti-particles, $\langle\sigma v\rangle_{e^\pm}$, for the mass of dark matter m_{dm} in the range of GeV to PeV. In order to calculate these, we have to exclude the integration term $\int_\gamma^\infty d\gamma_0$ from equation (1). Therefore, the electron and positron spectrum created by dark matter particles with a mass $m_{\text{dm}} \sim \gamma_0 m_e$ is given by

$$\begin{aligned} \frac{dn}{d\gamma}(r, \gamma, \gamma_0) &= \frac{1}{b(\gamma)} \frac{\exp\left(-\frac{r^2}{2\Delta\lambda^2}\right)}{(2\pi r^2 \Delta\lambda^2)^{1/2}} \times \left\{ \int_0^\infty dr_0 r_0 \exp\left(-\frac{r_0^2}{2\Delta\lambda^2}\right) \right. \\ &\quad \left. \times \left[\exp\left(\frac{rr_0}{\Delta\lambda^2}\right) - \exp\left(-\frac{rr_0}{\Delta\lambda^2}\right) \right] Q(r_0, \gamma_0) \right\}, \end{aligned} \quad (5)$$

where $r = 8.5$ kpc for the case of the solar neighbourhood. We then calculate the electron and positron spectrum for five different channels of annihilation, i.e. muon, electron, tau,

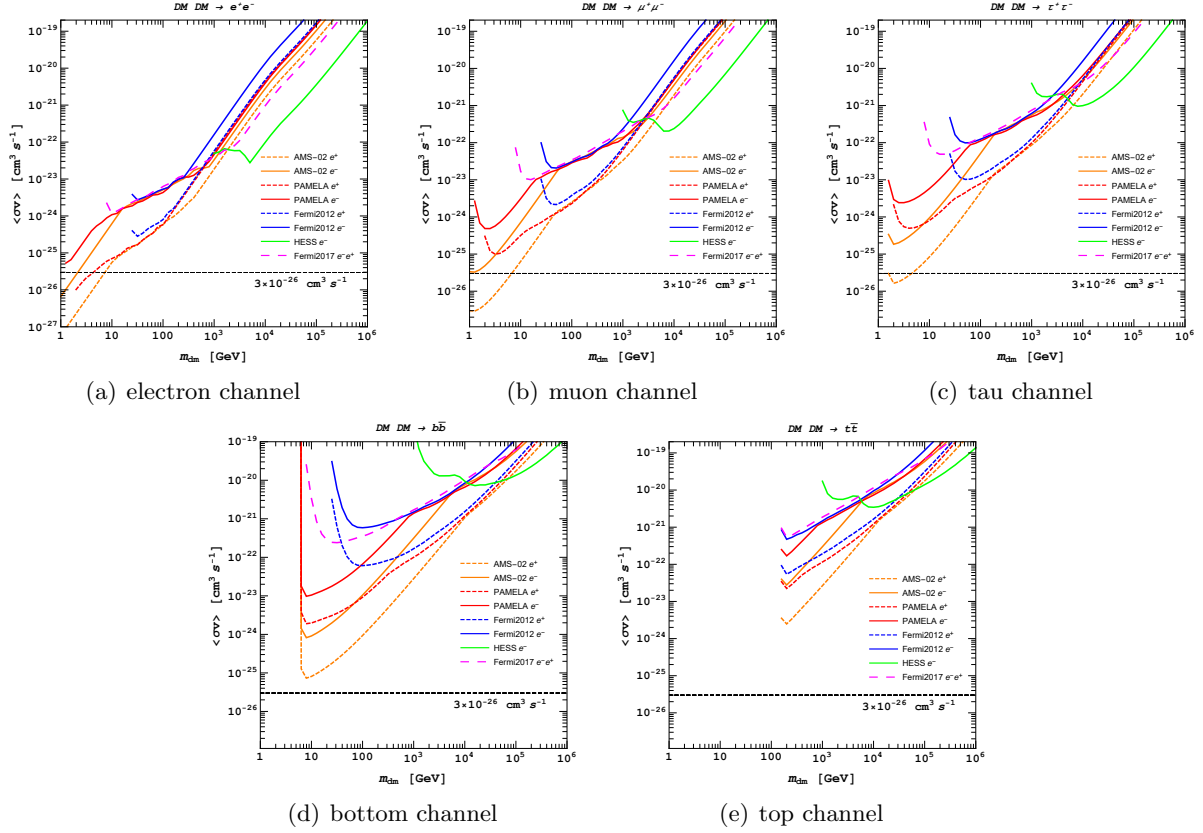


Figure 2. Upper limits of the cross-section of the annihilation of dark matter for electron, muon, tau, bottom and top channels derived from the various cosmic-ray electron and positron measurements.

bottom and top channels, which we adopt the final injection spectrum of positrons and electrons for each channel, $\frac{dN_{e^\pm}}{d\gamma}$ from PPC4DMID including electroweak corrections [12, 13], as we have mentioned in the previous section. Finally, the upper limits of the cross-section of the annihilation of dark matter $\langle\sigma v\rangle_{e^\pm}$ for each mass of dark matter m_{dm} and for each channel of annihilation is provided by constraining the parameter $\langle\sigma v\rangle_{e^\pm}$ to imposed that the model spectrum does not exceed the measured spectrum by AMS-02, Fermi-LAT, PAMELA and H.E.S.S.. We derive the upper limits within the mass range of 1 GeV to 1 PeV. The upper limits of the cross-section of the annihilation of dark matter for each annihilating channel are shown in figure 2 where the thermal relic cross-section, $\langle\sigma v\rangle_{e^\pm} = 3 \times 10^{-26} \text{ cm}^3 \text{ s}^{-1}$, is represented in the dashed-black line.

As shown in figure 2, our results indicate that for the electron, muon and tau channels, the cross-section of annihilation is lower than the thermal relic cross-section for masses of dark matter lighter than a few GeV. Therefore, the expected value for a thermal relic cross-section, described as $\langle\sigma v\rangle_{e^\pm} = 3 \times 10^{-26} \text{ cm}^3 \text{ s}^{-1}$, can be ruled out for these candidates of dark matter that have this lighter mass. For masses of dark matter that are lighter than $\sim 1 \text{ TeV}$, the lowest upper limit is provided by the positron data by AMS-02 whereas the electron spectrum by H.E.S.S. provides the lowest limits for dark matter masses larger than $\sim 1 \text{ TeV}$. The electron channel provides the tightest constraints for all measurements which give the upper limits for masses of dark matter between 10 GeV to 1 TeV about 1 to 2 order of magnitude higher than the thermal relic cross-section. As for masses of dark matter that are larger than $\sim 1 \text{ TeV}$, the

annihilation cross-sections are substantially higher compared to the thermal cross-section for all measurements and all annihilation channels, as also mentioned in [18–20].

4. Conclusions

Thus we have arrived at the upper limits of the cross-section of the annihilation of dark matter into positrons and electrons by using the cosmic-ray positron and electron data measured by H.E.S.S., AMS-02, Fermi-LAT and PAMELA. In our model, the propagation of the positrons and electrons is determined by a diffusion-loss equation which depends on diffusion, source term and energy loss rate. Consideration has also been given to self-conjugate dark matter particles with NFW profile in the Milky Way galaxy. The positrons and electrons are produced from the annihilation of dark matter through electron, muon, tau, bottom and top channels. After the production, the positrons and electrons travel through the Galaxy and lose their energy by inverse Compton scattering, synchrotron radiation and ionization. We have adopted parameters of the energy loss rate and the diffusion coefficient from the literature. The upper limits of the cross-section of the annihilation of dark matter can thereby be derived from the comparison of the predicted electron and positron spectrum for each annihilation channel with the observational data of positrons and electrons from cosmic-rays. The upper limits of the cross-section of the annihilation of dark matter for each dark matter mass are provided by imposing that the predicted values do not exceed the observational data.

The tightest limits on the cross-section of the annihilation of dark matter are derived from the positron data by AMS-02. Masses of dark matter smaller than a few GeV are excluded for the electron, muon and tau channels. However, the upper limits for the larger masses of dark matter particles are substantially higher compared to the thermal cross-section. The positrons and electrons produced from astrophysical backgrounds should be subtracted from the data before deriving the upper limits to get the better constraints.

Acknowledgments

S. Setthahirunin gratefully acknowledges that this research is supported in part by the Graduate Program Scholarship from the Graduate School, Kasetsart University. M. Wechakama would like to acknowledge that this research project is supported by Kasetsart University Research and Development Institute (KURDI).

References

- [1] Bertone G and Hooper D 2018 *Rev. Mod. Phys.* **90** 045002
- [2] Cirelli M 2012 *Pramana* **79** 1021
- [3] Aguilar M *et al* 2014 *Phys. Rev. Lett.* **113** 121102
- [4] Ackermann M *et al* 2010 *Phys. Rev. D* **82** 092004
- [5] Ackermann M *et al* 2012 *Phys. Rev. Lett.* **108** 011103
- [6] Abdollahi S *et al* 2017 *Phys. Rev. D* **95** 082007
- [7] Adriani O *et al* 2011 *Phys. Rev. Lett.* **106** 201101
- [8] Adriani O *et al* 2013 *Phys. Rev. Lett.* **111** 081102
- [9] Aharonian F *et al* 2008 *Phys. Rev. Lett.* **101** 261104
- [10] Wechakama M and Ascasibar Y 2011 *Mon. Not. R. Astron. Soc.* **413** 1991
- [11] Donato F *et al* 2004 *Phys. Rev. D* **69** 063501
- [12] Cirelli M *et al* 2011 *J. Cosmol. Astropart. Phys.* **1103** 051
- [13] Ciafaloni P *et al* 2011 *J. Cosmol. Astropart. Phys.* **1103** 019
- [14] Blumenthal G R *et al* 1986 *Astrophys. J.* **301** 27
- [15] Oh S *et al* 2010 *Astrophys. J.* **142** 24
- [16] Navarro J F, Frenk C S and White S D M 1997 *Astrophys. J.* **490** 493
- [17] Wechakama M and Ascasibar Y 2014 *Mon. Not. R. Astron. Soc.* **439** 566
- [18] Duangchan C and Wechakama M 2021 *J. Phys.: Conf. Ser.* **1719** 012012
- [19] Wechakama M and Khan Cantlay B 2019 *J. Phys.: Conf. Ser.* **1380** 012144
- [20] Khan Cantlay B and Wechakama M 2019 *J. Phys.: Conf. Ser.* **1380** 012071